UNIVERSIDAD TECNICA
FEDERICO SANTA MARIA

Departamento de Obras Civiles

WIND-EFFECTS ON BAR-BUILT ESTUARY HYDRODYNAMICS

Memoria de Título presentada por

Dhannai Tamara Sepúlveda González

como requisito parcial para optar al título de la carrera de

Ingeniería Civil

y el grado de

Magíster en Ciencias de la Ingeniería Civil

Profesor Guía
Megan Elizabeth Williams

AUGUST, 2022

UNIVERSIDAD TECNICA
FEDERICO SANTA MARIA

TÍTULO DE LA TESIS:

WIND-EFFECTS ON A BAR-BUILT ESTUARY HYDRODYNAMICS

AUTOR:

DHANNAI TAMARA SEPÚLVEDA GONZÁLEZ

TRABAJO DE MEMORIA, presentado como requisito parcial para optar al grado de MAGÍSTER EN CIENCIAS DE LA INGENIERIA CIVIL de la Universidad Técnica Federico Santa María.

Nombre Profesor Guía: Megan Williams

Nombre Miembro 1 Comisión: ....

Nombre Miembro 2 Comisión: ....

Valparaíso, Chile, September, 2022

WIND-EFFECTS ON BAR-BUILT ESTUARY HYDRODYNAMICS

Dhannai Sepúlveda[1], Megan Williams[1]

1 Universidad Técnica Federico Santa María

Abstract
Although bar-built estuaries are widespread on Mediterranean coasts all around the world, including central Chile, little research has been undertaken on its closed state, when its system is transformed into a salty lagoon. Understanding the dependence of hydrodynamic response and thermohaline-stratification on strong wind events and its associated transport and mixing is of prime importance on the impact of water quality and eutrophication on ecosystems in coastal lagoons. In this study, we analyze the role of external factors such as wind velocities, freshwater flow, and wave overtopping in the hydrodynamics of a shallow, highly salt-stratified bar-built estuary. Vertical mixing and forcing currents, governed by wind surface stress, were quantified for diurnal and hourly time scales.
Data collected in early 2012 at Pescadero Estuary, California shows that in a close state there is a strong stratification and strong wind events during its closed state and due to its morphology wind is channelized into the along-estuary direction, causing the lagoon to receive mainly local forcing. Frequency spectral analysis is used to identify seiches on the surface due to upwelling caused by the wind. Wavelet analysis was also used to identify wave overtopping on the sand bar and observe the real effect of saline water entering the estuary. During strong wind events, buoyancy frequency was reduced to almost 0 from the $0.1\ s^{-2}$ that the estuary usually had, and in some cases not return to its original value, showing upwelling and mixing of the water column. However, these effects varied over time depending on water level due to constant inflow from Pescadero and Butano creek. Some indicators like potential anomaly showed a good correlation with wind stress during the studied period. These preliminary findings show that wind effects are dominant in forcing vertical exchange of layers and generating currents at Pescadero.

Key words: bar-built estuaries, wind stress, stratification, upwelling, mixing

ACKNOWLEDGEMENTS

my acknowledgments

Contents

List of Figures

List of Tables

1 Introduction

By the definition of McSweeney et al. (2017) estuaries are "geomorphic systems which represent the transition between fluvial and marine environments". These coastal waterbodies such as fjords, bar-built estuaries, and coastal lagoons are constantly exposed to anthropogenic or natural disturbances due to their productive importance (Schernewski, 2002; Martínez et al., 2007) and global changes (Winckler et al., 2020). These ecosystems are exposed to sea-level rise, changing precipitation, and temperature patterns, in addition to a growing human population that is largely concentrated near the coast (Neumann et al., 2015). This type of habitat is highly variable and dynamic and is where complex physical and biochemical processes take place.

Bar-Built estuaries are systems characterized by periodic/intermittently inlet closure through a sand bar (Whitfield and Bate, 2007). These are mainly found in Mediterranean climates such as Chile, California, South Africa, and Australia (McSweeney et al., 2017). Closure occurs when a sand berm forms in the entrance channel and it can occur both seasonally or irregularly throughout the year (Behrens et al., 2013). However, it is common that annual variability dominates closure events due to the marked seasonal cycles for rain and river flow observed in this type of climate (Ranasinghe and Pattiaratchi, 2003). Despite the variable nature of these systems, they are vital for many species that have adapted to take advantage of the closed-mouth condition (Viaroli et al., 2008).

When the estuary inlet closes, external factors like wind, river flow, and wave overtopping can impact its structure. This could be causing changes in the density due to fresh and saltwater input or surface stress by wind effects, causing upwelling, mixing, or circulation changing the estuarine ecosystem (Ranasinghe and Pattiaratchi, 1999). The wind is the main external factor present, but the stratification makes it difficult to energize the denser layer, leading in some cases to a suppression of the turbulence under the pycnocline (Cousins et al., 2010). The foregoing makes these systems highly dynamic due to their variability in temperature and salinity, where complex physical and biogeochemical processes of oceanic and freshwater environments interact. Species that inhabit these types of environments are vulnerable to conditions such as hypoxia or anoxia in the lower layers (Kelly et al., 2018) or the retention of nutrients in the bottom (Cousins et al., 2010) and when there is upwelling or mixing it could happen abrupt changes for marine life and generate them some problems or even death (Marti-Cardona et al., 2008).

Previous research shows the response of the shear stress produced by the wind in large thermal-stratified lakes (Coman and Wells, 2012; Laval et al., 2008; Avalos Cueva et al., 2019), where it was observed how the wind stress affects these waterbodies when they have frequencies close to their natural oscillations and how the upwelling events caused by it cause variability in temperature. Even so, there is limited information on the hydrodynamic effects of the wind in small and saline-stratified lagoons, which would be interesting to study to learn how the wind affects their behavior and structure.

Currently, this type of estuaries is widely spread in Chile, because their seasonal conditions are similar to those of other places, already mentioned, where they are found, and despite this, there are few studies carried out in the country on the subject. In Dussaillant et al. (2009) an investigation was carried out on the Yali reserve, one of the most important wetlands in the central zone of Chile, whose knowledge must be complemented to fully understand the small and highly stratified coastal systems.

1.1 The Pescadero estuary

Pescadero Estuary is a small and highly stratified bar-built estuary located at the confluence of Pescadero Creek and Butano Creek on the California coast. It is located 60 [km] south of San Francisco Bay and 40 [km] north of Monterrey Bay (Fig. 1). The Mediterranean hydroclimate of Pescadero is characterized by an average annual rainfall of 750 [mm] with a cooler and more pronounced wet season that extends from November to April and a warmer dry season from May to October (U.S. Climate Data, 2021).

Figure 1: Location of Pescadero Estuary on California's Coastline. Images reprocessed from Google Earth.

The sand barrier placed at the inlet of Pescadero closes the estuary from the sea, changing its behavior to a stratified lagoon which usually happens during the dry season (Williams, 2014). Inlet rupture usually occurs during the wet season when precipitation increases flow and the lagoon fills to overflowing, leading to the scour of a new channel between the lagoon and the return of tidal action and seawater intrusions to the estuary (Largier et al., 2015). During periods when the mouth of the estuary is closed, the water level of the lagoon rises and could flood the surrounding marshy land.

The significance of this site lies in the detection of fish kills after the breaching of the lagoon mouth after an extended closure (Largier et al., 2015). Also, there are agricultural lands on the surroundings that have a productive importance for the local community in addition to other concerns as winter flooding of low-lying lands, in which exists some roads and parts of the town, or the presence of a wide diversity of habitats and microhabitats in the estuary.

Pescadero has two main water inputs: freshwater inflow and saline water, which sometimes get mixed and other times form a two-layer structure. The behavior of the estuary depends on the mouth state, where we can observe an 'open' and 'closed' state. Pescadero receives freshwater inflow from two relatively small watersheds, which have a highly variable discharge, following precipitation that varies from day to day through the wet season, as well as seasonally and between years (Largier et al., 2015). The Pescadero watershed is about twice the size of the Butano watershed, and produces 57% of the streamflow (Williams, 2014). On the other hand the Northern Californian coast experiences a semidiurnal tide with a neap tide range of under 1 m and a spring tide range up to almost 3 m (Williams, 2014). Saltwater get into the estuary easily during open state, but when the inlet is closed seawater has to overtop the sandbar to get into the estuary, which happens occasionally during high tide and strong waves.

When the mouth is closed the estuary takes a stratified structure fed by the freshwater input and the sporadic wave overtopping saline water. In this form is more difficult to energize the water column, but it can happen with external factors as wind stress in the surface or from the discharge and the wave overtopping. However, vertical transport in Pescadero couldn't be from density-driven exchange, because the estuary would be always saltier than the creeks input water, so it always will stay on the top of the water column making the estuary stratified. Even that, in Pescadero there is a light density/salinity gradient due to the freshwater input upstream and the saltwater overtopping the bar at the other end.

1.2 Motivation

In its state of disconnection from the ocean (i.e., closed state), the estuary can take the form of a shallow stratified lagoon, due to the presence of saltwater and freshwater from fluvial inputs (Behrens et al., 2016). This estuary state could lead to eutrophication if there are no energy inputs to the system (Nunes and Adams, 2014), and usually, the wind is the main source, driving to mixing and destratification in small bar-built estuaries ((Gale et al., 2006)) triggering processes that impact mixing and circulation, which could affect the marine life of the estuary ((Marti-Cardona et al., 2008)).

As said before, the wind is the principal driver of mixing present, but sometimes stratification makes difficult to energize the denser layer, leading in some cases to suppression of turbulence below the pycnocline (Cousins et al., 2010). This could cause hypoxia or anoxia in the lower layers (Kelly et al., 2018) or retention of nutrients in the bottom (Cousins et al., 2010) and when there is upwelling or mixing, abrupt changes could occur for marine life and generate problems or even death (Marti-Cardona et al., 2008).

Due to the latter, these waterbodies are highly dynamic, and this makes them sites of great importance for research. On the other hand, estuaries are the connection between the earth and the ocean, receiving waters coming from rivers and creeks that are exposed to anthropogenic effects, causing changes in freshwater flow or temperature, in addition, to being subjected to sea level rise and wave climate variations (Winckler et al., 2020; Holt et al., 2010; Thorne et al., 2021). Besides, in the estuaries, of their contact with the coast and rivers, activities such as fish farming or agriculture are developed, so they have economic and social importance to communities.

The response to strong and sustained wind stress in a closed state bar-built estuary starts with a setup of the surface and a change in the pressure gradient. This will cause the pycnocline to tilt upwards at the upwind end of the estuary leading sometimes the bottom layers to rise to the surface. The reduction or end of this wind forcing releases the pycnocline from its tilted position and return to horizontal. The upwelling effect caused by wind forcing has potential relevance in nutrient and oxygen exchange between layers (Kelly et al., 2018) and has been studied widely in lakes using temperature measurements (Coman and Wells, 2012; de la Fuente et al., 2010; Roberts et al., 2021), however, there are fewer studies that observe this kind of behavior at bar-built estuaries or in smaller coastal lagoons.

2 Objectives

2.1 General objective

The mean goal of the present work is to study velocity and density variability in the water column of a small and highly stratified estuary during its closed state and relate them to wind stress, to use the collected information to delve into the study of water bodies of this type. In addition, this research seeks to gain a better understanding of the relationship between wind stress and the behavior of layers of different densities within the closed state estuary. Our case study is the Pescadero Estuary, a bar-built estuary in California that represents many other small inlet systems elsewhere in the world. Data sets of wind and pressure at this site containing several mouth openings and closures are going to be used.

2.2 Specific objectives

The specific objectives of this study are:

(1) To make a time-series analysis of data collected from the Pescadero estuary using depth, temperature, salinity, and velocities collected from the estuary and the wind velocities obtained at 3 meters height.

(2) To determine the effect of wind stress on the hydrodynamic characteristics of the estuary while the inlet is closed focusing on stratification.

(3) To study the wind-estuary interaction and the effects of other external factors such as water inflow and wave overtopping in this interaction.

3 Literature review

3.1 Bar-built estuaries in the ecosystem and the community

Climate change is affecting multiple marine ecosystems globally (Hewitt et al., 2016). Its been detected that the global oceanic oxygen content has decreased during the last five decades (Schmidtko et al., 2017) and that air temperature is increasing in oceans (Omstedt et al., 2004; Jones et al., 1999) which according to models can affect stratification in northwest European continental shelf and Baltic Sea due to a decrease of salinity at the surface (Hordoir and Meier, 2012; Holt et al., 2010) changing the number of days that stratification is present causing impact in nutrient flux. Also, some studies expect that the absolute mean sea level on Chilean coasts rises between 0.35 to 0.74 m in the next 80 years (Winckler Grez et al., 2020). The effects of climate change can put at risk the coastal zones, including estuaries and coastal lagoons which are especially abundant ecosystems in flora and fauna.

In addition, there is evidence that there is a decrease in surface wind speeds in Northern Europe (Woolway et al., 2017) and an increase in along-shore winds in the Chilean coastal zone (Winckler Grez et al., 2020). It is known that changes in surface wind speed affect the number of days that a lake is stratified, which affects the nutrient availability and quality of a waterbody, changing the amount of oxygen present in deep waters (Woolway et al., 2017). It is important to study wind effects in estuaries to be able to quantify how wind-speed changes will affect these environments.

In central Chile, there is a decrease in river discharges affecting buoyancy and stratification (Winckler Grez et al., 2020), which can be causing a wide range of changes in estuarine and marine ecosystems, including changes in oxygen availability. These changes can impact fish populations and other autotrophic organisms.

The importance of intermittently closed estuaries goes beyond local impacts. These estuaries can accumulate sediment and minerals while the inlet is closed (Thorne et al., 2021), and in rainy seasons they open the mouth naturally because of the increase in freshwater inflow (Hoeksema et al., 2018). This process settles sediments to the near marshes helping to maintain their elevation according to the sea level, mitigating the consequences of sea level rise (Thorne et al., 2021). On the other hand, it is very common opening the mouth artificially to avoid flooding the near lands (Behrens et al., 2013) which doesn't allow the sediments to set correctly in the marsh platform (Thorne et al., 2021). ENSO (El Niño Southern Oscillation) is the principal cause of the opening and closure of the mouth (McSweeney et al., 2017), but this phenomenon can change its occurrence in the next years, affecting estuaries' dynamics and water quality all around the world (Thorne et al., 2021).

Climate change is affecting bar-built estuaries' dynamics and water quality. Increasing river discharge due to more precipitation could lead to increase erosion and the number of suspended particles of sediment in the water. Enhanced sediment concentration could lead to accumulation in the estuary making the inlet close, changing the equilibrium of opened and closed state of the sand bar, which along with the increase of freshwater input could flood the surrounding land (Peeters and Kipfer, 2009). Consequently, depending on the vegetation present and its oxygen demand, deep-water oxygen may be reduced or suppressed (Kelly et al., 2018; Largier, 2021). Also, the density of the surface waters will be reduced and thus could change the estuary behavior to external factors such as wind stress.

On the other hand, bar-built estuaries are under continuous anthropogenic stress due to their closeness to human settlements (Clark and O'Connor, 2019) and their productive importance. Dams constructed upstream for water storage reduce the freshwater that goes to the ocean, causing the retention of suspended sediments. This results in a change in the morphology of the estuary due to not receiving the sediments that used to accumulate in the inlet, leading to premature scour of the sand bar (Peeters and Kipfer, 2009). Also, to prevent the flood of roads or agricultural lands that settle nearby, the community plan the opening of the inlet artificially, which could result on abrupt changes on the estuary ecosystem Behrens et al. (2013).

3.2 How bar-built estuaries are studied in Chile and around the world

There are plenty of methods and instrumental techniques to measure the behavior of estuaries and lakes at a small scale (Wüest and Lorke, 2003), methods that can be used with new data and get improved for future works and be more specific for the different types of waterbodies. McSweeney et al. (2017) studied the bar-built estuaries all around the world and their climatic, marine, and fluvial conditions to classify them and quantify the drivers of their distribution in each continent. That can "allow predictions of estuary response to climate change and human impacts to be made and to ultimately assist with integrated coastal management into the future".

Dussaillant et al. (2009) studied a Chilean coastal lagoon in its open and closed state and observed that in its closed state the rainfall influence was not important except for the storms that open the inlet to the sea. He also observed that wind is very important in water level fluctuations in the disconnected phase. He studied the connected phase using a general pattern, spectral, and Fourier analysis.

Kelly et al. (2018) observed that in stratified waterbodies, when the vertical exchange is limited, it can be oxygen depletion present, causing hypoxia and anoxia, a factor that is related to fish kills in Pescadero (Largier et al., 2015). Kelly et al. (2018) proposed that tidal influence oxygenated the deeper layers in a saline lagoon in some specific events and observed that the same conditions were present when there was wind-driven upwelling, showing a relation between tidal influence and wind stress in vertical mixing.

Behrens et al. (2016) observed the salt intrusion in a bar-built estuary and its differences between closed and open state conditions. The study found the presence of alternating shallow sills and deep pools, which act to trap the salt after intrusion, and suggested that internal seiche motions in the outer estuary initiate the intrusion by lifting saline water in the pycnocline high enough to crest the sills. This salinity intrusion extends to distances of several kilometers from the beach.

Studies carried out in Rodeo Lagoon (Cousins et al., 2010), a shallow strongly-stratified lagoon, found that stratification by brackish water leads to a pronounced suppression of turbulence below the pycnocline and confines nutrients released from the sediment into the lower layer. Those can be confined for up to several months, compared to the rapidly flushed overlying fresh layer. They observed that in the lagoon wind is the dominant source of mixing because of a lack of other energy inputs and destratification by wind mixing allows for the redistribution of nutrients from the bottom brackish layer.

3.3 Pescadero estuary studies

Pescadero estuary has literature related to management plans focusing on productivity (Curry et al., 1985) or in preserve the hydrology of the estuary (Williams et al., 1990). But recent studies have been motivated on the fish kills that have been observed in the last years, signaling that when the sandbar closes stratification leads to the creation of an anaerobic environment in bottom waters (Sloan, 2006). Also, geochemical analysis to sediments showed that the transition from closed to open state leads to poor water conditions within the Pescadero Estuary, with many indicators reaching values that are outside the range of optimal conditions for fish or aquatic life (Richards et al., 2018).

In addition, it has been studied more physical phenomena like the effects of the constriction that generates the mouth in its open state, showing a discontinuous tidal forcing in the estuary (Williams and Stacey, 2016). Williams and Stacey (2016) observed that wave setup and tides set the estuarine water level, while the mouth sandbar limits ocean gravity waves to enter the estuary but permits infragravity motions to pass through the inlet, which induced energetically important high velocities, highlighting the strong dependence of hydrodynamics of small bar-built estuaries on nearshore processes. Also, hydrodynamic processes in Pescadero are comparable to similar estuaries along the western coast of the Americas as well as in Australia, South Africa, and in estuaries in Mediterranean climates on the Atlantic west coast of Europe, as well as in shallow sandy inlets elsewhere.

4 Methods

4.1 Field observations

Four field campaigns were carried out between 2010 and 2012 described in the work of Williams (2014) and Williams and Stacey (2016), but in this work, we will focus exclusively on the data between January and March 2012 to analyze the behavior of the estuary in a closed state. Measurements were made using instruments for speed and depth, as well as including a meteorological station to collect wind speed and direction data. Depth data were collected using moored pressure, conductivity, and temperature sensors (CTD) placed at different heights and distributed along the estuary at four points as shown in (Fig. 2), called Near Mouth (NM), Mid-Lagoon (ML), Deep Channel (DC), and Pescadero Creek (PC). Density profiles were made on February 16th with a CTD logger around 5 p.m. at the locations indicated in Fig. 2. The moment the profiles were made the wind was calm, so is not causing a disturbance in the water.

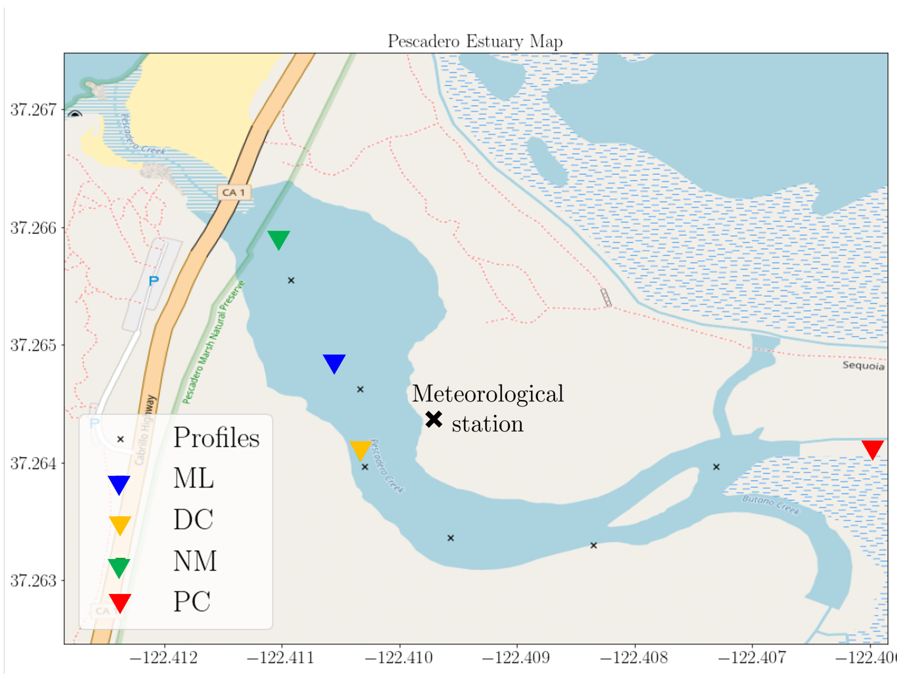

Figure 2: Pescadero estuary map and location of the sensors (NM: Near Mouth, ML: Mid-Lagoon, DC: Deep Channel and, PC: Pescadero Creek), instant profiles, and meteorological station.

Velocity measurements were made with an Acoustic Doppler Current Profiler (ADCP) anchored to the bottom of the estuary at location DC. This instrument is designed to be used in deeper water, so data collected from the surface could be affected by the interference caused by reflection. Due to the latter, the data from the surface were removed from the record. On the other hand, the ADCP has a blank space at the bottom for measuring speed, so the first measured point was 71 cm above the ground, meaning there is only a window of velocity data in the water column.

For wind speed data, an anemometer was installed 3 m above the water level in marshy land adjacent to the estuary (Fig. 2). It was observed that due to the topography of the sector, the wind direction is channelized along the estuary, so the wind goes mainly bidirectional. Directions between 300 and 360 degrees come from the ocean and the wind that blows from 100 to 170 degrees comes from inland.

To complete the information, the freshwater streamflow into the Pescadero estuary is estimated based on a United States Geological Survey (USGS) gauge located on Pescadero Creek 8.5 km upstream from the mouth of the estuary (USGS 11162500) (Water Data, 2022). The tide height data in San Francisco Bay and Monterrey Bay (stations 9414290 and 9413450 respectively) were obtained from the National Oceanographic and Atmospheric Administration (NOAA) (Tides and Currents, 2022b,0), and waves data were obtained from the National Data Buoy Center, 40 km in the ocean from the coast of Half Moon Bay (station 46012) (National Data Buoy Center, 2022). Additionally, the bottom pressure measurements at each sensor were corrected for sea-level atmospheric pressure measured at the nearest weather station located at the Half Moon Bay airport. This work focuses exclusively on the two periods where the estuary is closed between February and March.

4.2 Data processing

4.2.1 Salinity and temperature

The CTDs measurements were made with a frequency of 10 or 30 sec, and at each location, there were one (PC), two (ML), three (NM), or four (DC) instruments at different depths, hence, we don't have a complete salinity or temperature profile in time and we don't know where the interface between the saltiest and the sweetest layer of the estuary lies. We obtained the density using the salinity, temperature, and pressure data, by the GSW Python package which is an implementation of the Thermodynamic Equation of Seawater (TEOS-2010).

Additionally, there were taken CTD profiles on February 16th, between 17:00 and 17:30 which were used to calculate the density also using TEOS-2010. When the profiles were taken the wind was very calm so we can say that the estuary was not having any significant external forcing.

Temperature is an important parameter for density, notwithstanding salinity stills dominates density values, there are a few points we must aboard about temperature in Pescadero. First, horizontal temperature gradients are present in Pescadero, where upstream is warmer meaning the water coming from the creek is warmer. In addition, during the studied period, the water temperature in San Francisco buoy from the National Data Buoy Center was between 9^oC and 11^oC, so the water coming from the sea will be colder. Second, the temperature in the estuary is colder on the surface and warmer at the bottom, probably since is winter during the studied period and the temperature in the air is lower than in the water coming from upstream. The coldest temperature can be on the surface without sinking for being denser because salinity dominates density in this case. Third, Pescadero in its closed state takes the form of a shallow lagoon, meaning that is more prone to heat loss and air temperature than other bigger lakes (Peeters and Kipfer, 2009).

To represent stratification we used buoyancy frequency, defined as $N^2 = -(g/\rho)(\partial\rho/\partial z)$ (Kundu and Cohen, 2002) representing the water column stability, which increases or decreases as the fluid is more or less stratified. The potential energy anomaly was calculated to observe the behavior of density in the water column. It represents the work per volume required to completely mix the water column and is calculated using the equation shown by Simpson et al. (1985):

$$\phi = \frac{1}{h}\int_0^h (\bar{\rho} - \rho) gz dz \tag{1}$$

which we discretized according to the number of sensors that each location had and considering each layer's limits as the corresponding upper and lower sensors and the density for the whole layer as the upper one.

4.2.2 Estuary currents

Velocity data collected with the ADCP were axis-rotated to the principal coordinates ($u - v$), based on its direction of maximum variance as shown in Fig. 3. This was calculated for the studied period, obtaining an angle of 48.6^o from the west axis in a clockwise direction and it was established that the velocity was positive in the direction of the flow (u), that is, towards the sea.

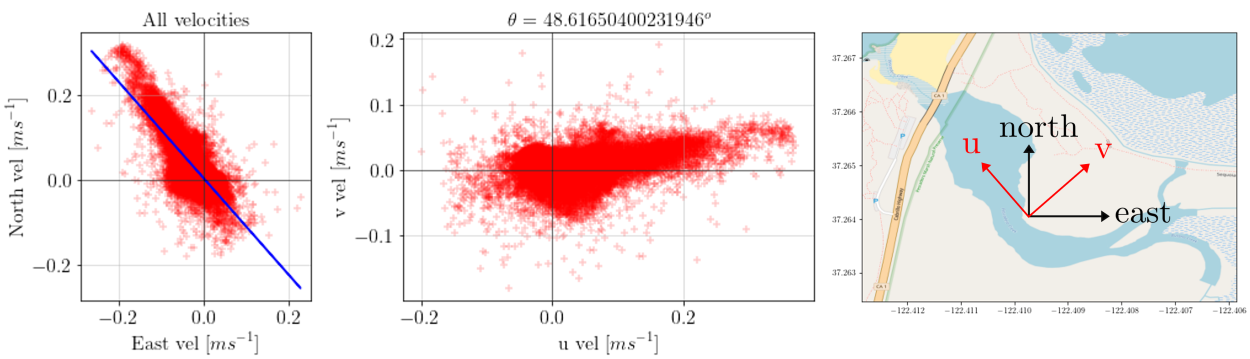

Figure 3: Speed data plotted in North-East and $u - v$ coordinates, and a map of Pescadero signaling the coordinates.

ADCP data were averaged every 5 minutes to take off high-frequency signals. However, CTD data at the same location (DC) was not measured at the same depth due to bathymetry, thus we estimated the difference between both and adjusted the first cell to 0.91 m above the bottom of the estuary.

4.2.3 Wind stress

Wind velocity data were also axis-rotated to the principal coordinates of the estuary currents, with an angle of 48.6^o. Also, we calculated the wind shear stress above the surface using the equation from Read et al. (2011)):

$$\tau = \rho_{air} C_D U_{10}^2 \tag{2}$$

Where ρ_{air} is the specific weight of air (1.2 kg/m^3), C_D is the drag coefficient and was defined by Large and Pond (1981) at 0.0012 for wind velocities between 4 and 11 m/s, and considering that the collected speeds are smaller than 11 m/s and the results are not sensitive to C_D it was set as 0.0012. U_{10} is the adjusted wind speed at 10 meters high, and it was obtained by:

$$U_{10}^2 = U_z * (1 - \frac{C_D}{\kappa} * \ln \frac{10}{z})^{-1} \tag{3}$$

with $\kappa = 0.4$ as the Von Karmann coefficient and z = 3 m.

To study the response of the stratified layers to a wind impulse and identify the upwelling we used the Wedderburn number (Shintani et al., 2010):

$$W = \frac{g' * h_1^2}{L * u_*^2} \tag{4}$$

where we estimated h_1 as the 30% of the DC's total depth, L as 392 m, and for u_* and g' we used:

$$g' = \frac{\rho_{bottom} - \rho_{surface}}{\rho_{surface}} * g \tag{5}$$

$$u_*^2 = \frac{\tau_w}{\rho_{surface}} \tag{6}$$

To analyze the relationship between wind stress and density we standardized and normalized the signals and applied cross-correlation. Cross-correlation between wind stress and density signals is used to find the time lag (phasing) between both and their level of correlation along the locations (propagation) measured in the estuary. Also, we can compare the results to the response tilt time that can be considered as $1/4$ of the internal wave period T_1 (Stevens and Imberger, 1996):

$$T_1 = \frac{2L}{\sqrt{(\frac{\epsilon g h_1 h_2}{h_1 + h_2})}} \tag{7}$$

4.2.4 Water level

To analyze what was happening on the surface, a frequency spectral analysis was carried out in order to identify the most important processes that affect the water level. First, Welch (1967) method was applied to reduce the data noise and there was applied a detrend. Finally, the signal was multiplied by a quadratic window to obtain much clearer data and then apply the frequency spectral analysis.

To complement this information, an analysis of the wavelet transform was carried out using the Python package PyWavelets (Lee et al., 2019). The one-dimensional continuous wavelet transform was applied to the DC surface height data using the first-order Gaussian derivative family for a period range between 10 s and 2.8 min. This, in order to identify important events and other external phenomena, such as a wave overtopping the sandbar due to high tide. This analysis delivers coefficients that are a function of scale and position and that serve as a scalogram to visualize the wavelet.

To carry out a more detailed visual analysis, the standardized heights were obtained at the NM and DC points, where the difference between their real value and their average was obtained, in order to compare the results of both on the same scale. In addition, the difference between the two was calculated and amplified by 10 to exaggerate its trend and observe it more clearly.

All the mentioned data were plotted according to local time, to analyze visually considering the factors that affect day and night as temperature and wind. Abrupt decreases in water level that were proceeded by a slow increase in the estuarine water level without tidal influence were defined as mouth openings and when tidal energy is not visible at the water level there is a mouth closure. We observed that the inlet opened twice and each time there are abrupt density changes in the water column.

5 Results

5.1 Conditions observed during closed state

5.1.1 Wind in the estuary

In Fig. 4 we can observe that the wind is mainly bidirectional and when it goes onshore the magnitude is bigger. This form is due to the topography of Pescadero which have an escarpment at the south of the inlet, protecting the mouth. Also, the marsh itself is located in a low valley, constricting wind flow paths. For the along-estuary velocity (u) we observe that the maximum velocities reach until 10 and -10 m/s approximately (Fig. 5). In the cross-estuary velocity (v) we observed just a few spikes where the maximum velocity was reach, at approximately 5 and -5 m/s.

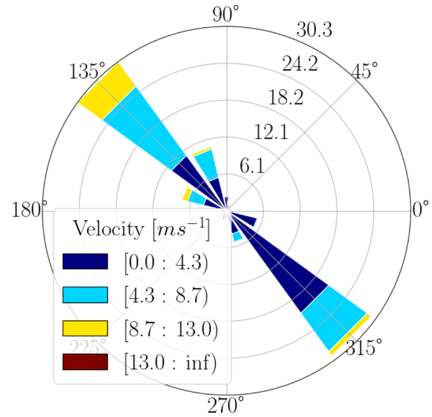

Figure 4: Windrose of the data collected in Pescadero from Jan 15th to March 20th.

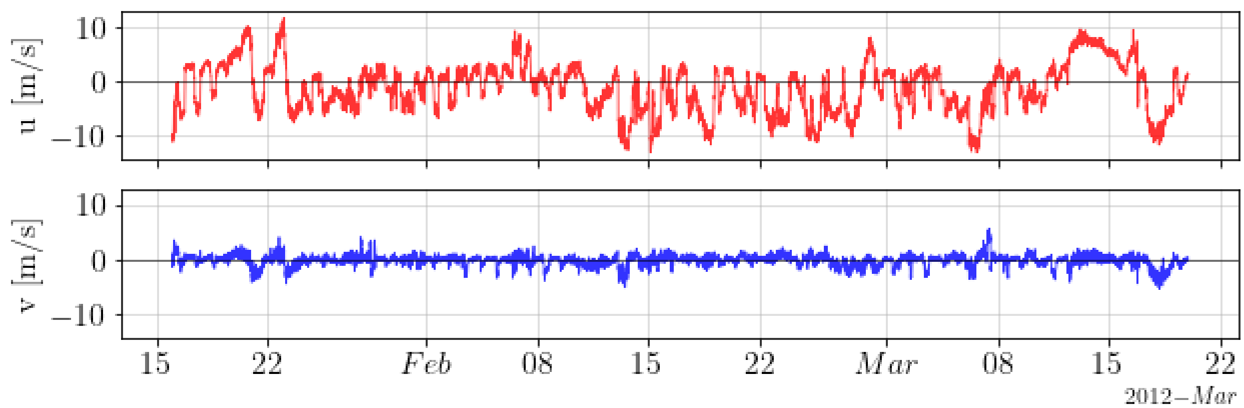

Figure 5: Time-series of wind speed in u and v direction.

5.1.2 Evolution of density structure

Pescadero estuary is characterized by having a strong thermohaline stratification in its closed state (Fig. 6). When the estuary inlet starts closing, temperature and salinity acquire different values on the top and bottom of the lagoon, increasing density change in the vertical (Largier et al. (2015)). The sand bar that forms at the inlet of the estuary contains the freshwater inflow and does not allow the waves to enter, but during high tide the waves could be overtopping it (Laudier et al. (2011)), contributing to the salinity in the system. This, depending on the magnitude of the intrusion, could affect the stratification of the entire estuary.

We defined closed state at the estuary when the depth's change in time $\Delta h/\Delta t$, with $\Delta t = 10$ hours, is positive and less than 0.01 m/h for more than a day (Fig. 6), meaning that the lagoon is filling with freshwater, increasing its level, and with a low influence from the sea. In that context Pescadero is in closed state three

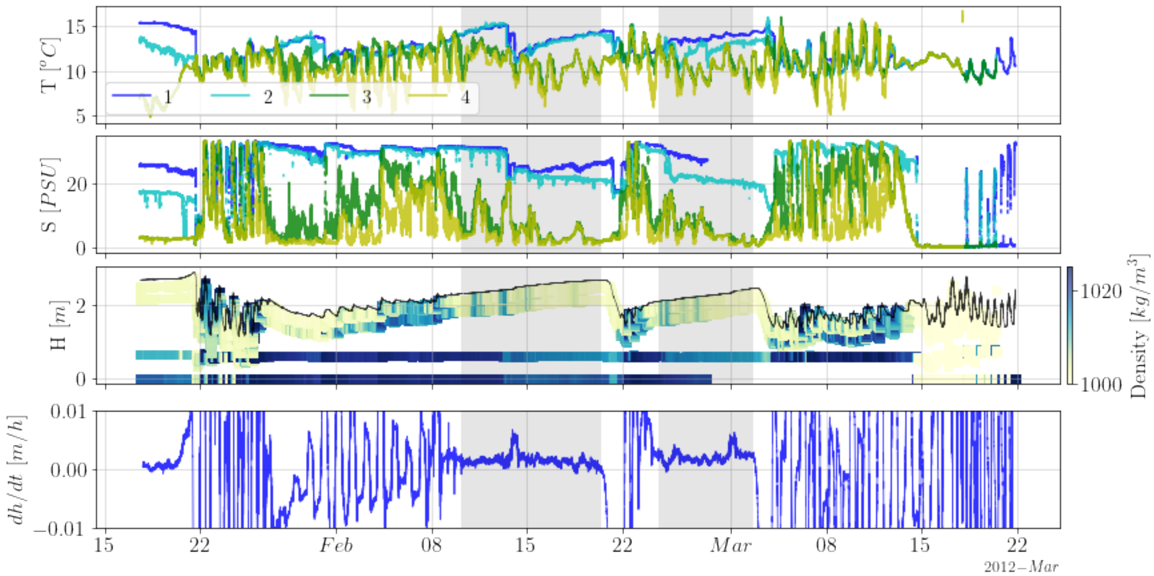

Figure 6: Time-series windowing at both closure phases of temperature and salinity in NM, where 1 is the deepest sensor and 4 the shallowest, colormap of density in NM in the water column, where the black line represents the water level, and the change of the water level in a 10-hour frame.

times, in mid January, in mid February, and in late February/early March where the first is at the start of the time series, not including the initial closure, while the second and third are in gray shadow (Fig. 6). The differences between these three closures are that the first has the highest water level, and second and third closures never get to the same level.

It is known that the first breach of the bar was artificial (Williams (2014)), openings that according to Behrens et al. (Behrens et al. (2013)) would be less effective in keeping the mouth open than those that developed naturally, as in this case when the estuary is in open state for just a couple days. The second barrier breach is believed to have occurred naturally.

In the time series we observed during closed state the temperature and salinity went stratified (Fig. 6). We observed a lower and non stable temperature at the surface (Sensors 3 and 4 in Fig. 6) due to the cold season and the following of day-night temperature changes. The temperature at the bottom (Sensors 1 and 2 in Fig. 6) is more stable, but still being influenced by daily changes and other external factors, indicating for example an abrupt fall on February 13th, and then started to increase again. The bottom salinity is also steady most of the time and is generally decreasing. The surface salinity is more vulnerable to external factors, and only is more stable during closed state.

During closed state, we observed three layers in the density structure with the superior one getting thicker upstream. In Fig. 7 there is the longitudinal view of the estuary densities from the profiles and the moorings. We can observe that in near the mouth the salinity is higher or the water column is more homogeneous. After a few days in closed state, the estuary opened on February 21st and March 3rd observing a decrease in water level.

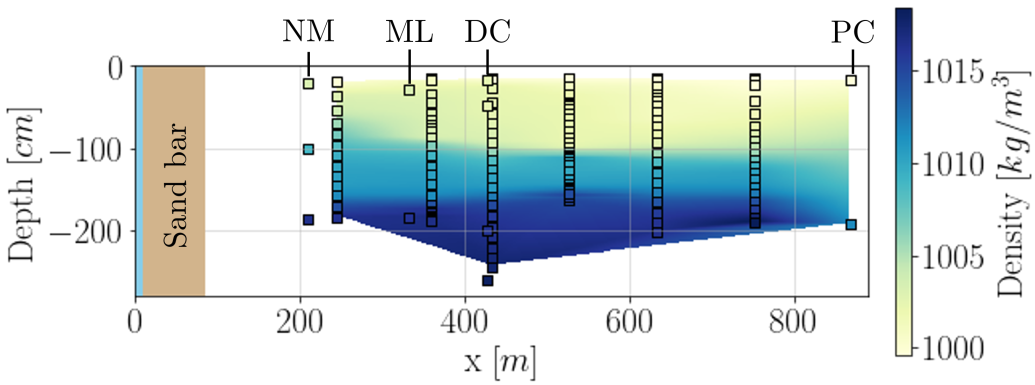

Figure 7: Along-estuary density colormap of Pescadero. Distance x is considered from the coast following the curvature of the estuary as the sensors are placed in Fig. 2.

5.1.3 Tidal and waves conditions

In Fig. 8 we have the wave conditions for Pescadero during the study period. We can observe, that when the mouth is open tidal influence is present in Pescadero, but when the mouth closes we cannot observe an evident effect at plain sight, which does not mean there is not present. Significant wave height goes from 2.5 m to more than 5 m approximately, but we have to account that deep water wave heights are larger than wave heights experienced at the coast (Williams (2014)), and as this data where collected 40 km from shore, thus we use this value as a proxy for coastal ocean conditions.

The rest of the parameters (wave periods and direction) were collected for the same buoy, so they also are an approximation of the wave conditions. Dominant periods go from 5 to 20 s, while averaged periods have al range only between 7 and 10 s. Direction of the dominant period is stable around the 300 degrees most of the time, with just a peak on February 29th where reaches the 250 degrees.

5.1.4 Pescadero creek discharge

Pescadero estuary receives freshwater from Butano Creek and Pescadero Creek, where the latter is the one that contributes the most to the lagoon and the one we have available data. When the inlet is closed, the maximum flow recorded was $0.72 m^3/s$, lower than the usual for winters in California, presenting two small increases in flow (Fig. 9), but which, due to their low magnitude, would not be a determining factor in the rupture, considering that between July 2011 and July 2012 the maximum flow was $29.73 m^3/s$. Even so, there is a constant inflow of fresh water that increase the estuary water level progressively until the inlet breaks.

5.1.5 Currents speed and direction

During closed state, the wind direction is predominantly onshore and its magnitude in that direction is bigger than in the rest of the period (See Fig. 5). Surface wind stress over the closed estuary causes the upper layer to go in the same direction as the wind, and the lower layer to move in the opposite direction. Given the limitations of the ADCP sensor, velocities near the surface were not always captured, therefore, we observed a range of speed, not showing what happens at the bottom or the surface. Pescadero has its main directions very marked, case that is very particular in this kind of estuaries, where along-estuary velocities always domain the

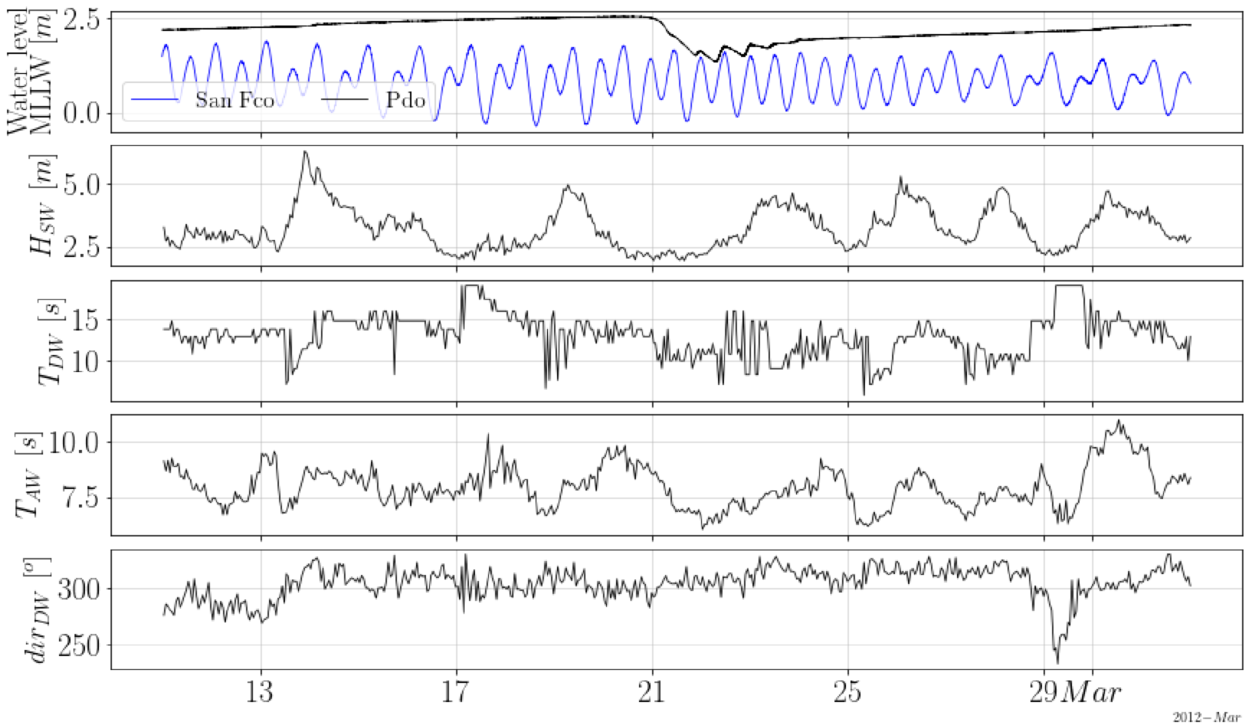

Figure 8: Time-series of tidal height in San Francisco (blue) and Pescadero estuary water level (black) in MLLW datum, significant wave height (H_{SW}), dominant wave period (T_{DW}), average wave period (T_{AW}) and the direction from which the waves at the dominant period are coming (dir_{DW}).

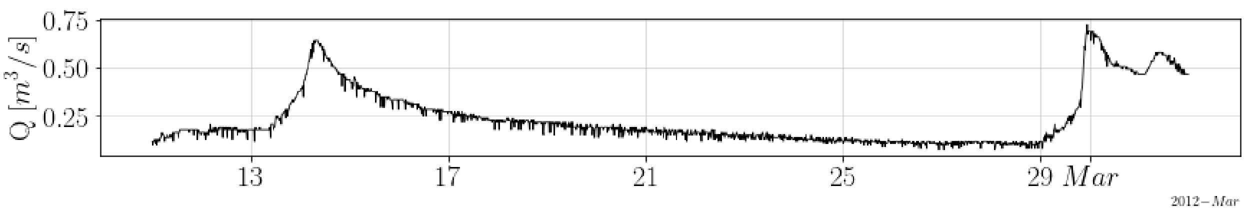

Figure 9: Time-series of freshwater flow from Pescadero Creek.

currents (local forcing).

5.1.6 Surface fluctuations

We can observe, that when the mouth is open tidal influence is present in Pescadero, and when significant wave height increases the influence is also larger (Fig. 8). When the bar blocks the inlet, this causes accumulation of the upstream freshwater in the lagoon which is represented as an increase in Pescadero water level, reducing the ocean influence to be negligible to plain sight, but still could be wave overtopping. This wave overtopping can be detected by the fluctuations in the surface present in the data, but also we have to consider the fluctuations caused by wind stress or by an increment of the discharge.

5.2 Hydrodynamic controllers

The external factors that could be affecting the estuary in closed state are freshwater inflow, saltwater intrusion, and wind stress. There are other factors involved as temperature or evaporation, but we estimated that those were negligible due to the haline stratification that dominates the estuary structure.

5.2.1 Stratification controllers

At the beginning of both periods of disconnection, we noticed that there were changes in densities on the surface and in the deep layer, although the latter in smaller magnitude and fewer times (Fig. 10). Three important wind events occurred in each period that matches with the increase in surface densities, observing that when the stress on the surface increases, so does the density in the upper layer in the three sensors. When wind forcing decreases, we noticed that density tends to return to its initial state, except for the largest events at the beginning of both periods, where density at the bottom is smaller after the event than before.

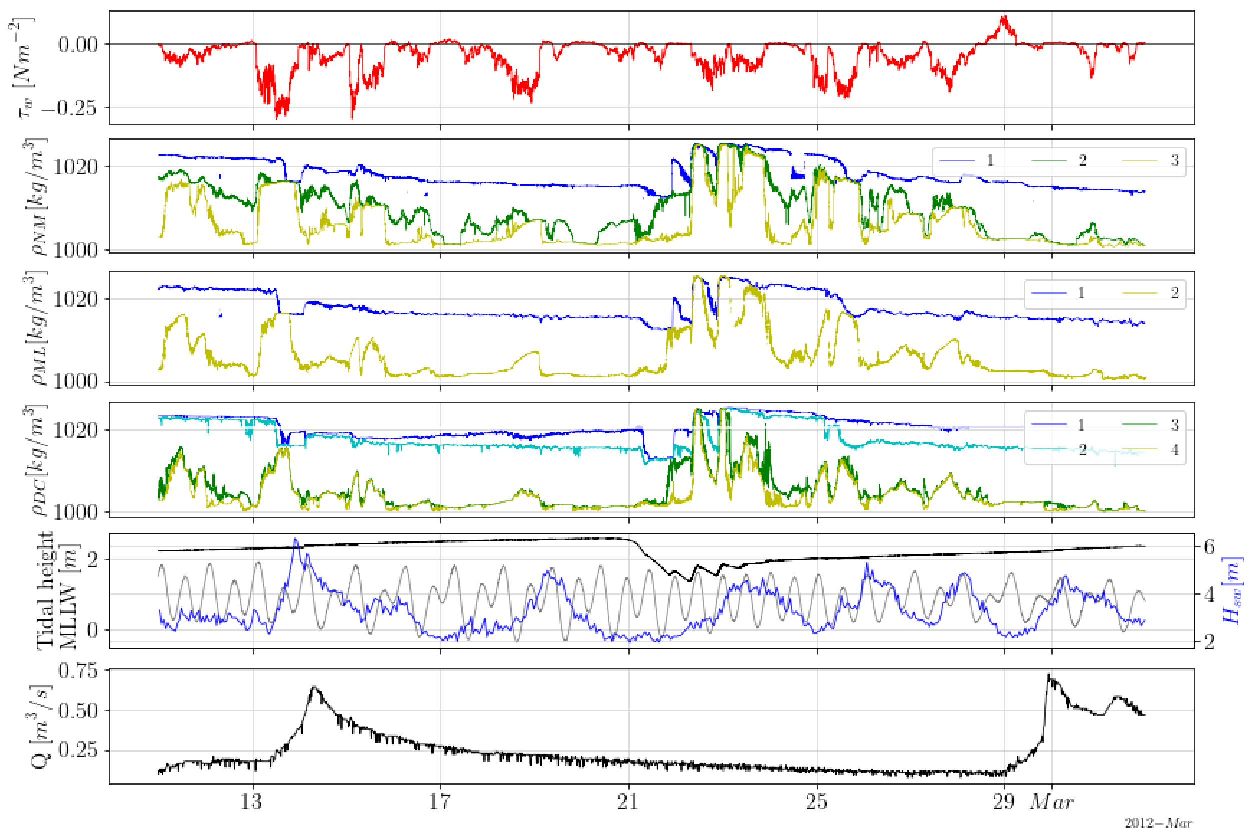

Figure 10: Time-series of wind stress (τ_w), NM (ρ_{NM}), ML (ρ_{ML}) and DC (ρ_{ML}) densities in different depths, where the sensor 1 is the deepest and the sensor 4 is the shallowest (The positions in the water column of the sensors are showed in Fig. 7), significant wave height in Halfmoon Bay in blue (H_{sw}), Pescadero estuary water level (black) and tidal height in San Francisco (gray) in MLLW datum, and freshwater inflow of Pescadero creek (Q).

Upstream inflow had two increasing events in the studied period (Fig. 10) and during those events, there wasn't an instant change in density, but we can notice that there is a trend in density, especially in the lower layers, where density is decreasing in time in both disconnected periods in NM and ML. In the first period, at DC location, different to the others, there is an increasing trend of density, which would not be unusual considering the lower layer of DC is much deeper than the ones of NM and ML (Fig. 7), and the layer in DC with the same depth to those is the one before the deeper (in cyan, Fig. 10). Another change in density that is noticeable occur in the middle layer of NM (in green, Fig. 10) between February 13th and 17th, just before and after there was an increase in discharge, where density started at around 1015 kg/m^3 and ended at almost 1000 kg/m^3.

Significant wave height and tidal height could be showing some wave overtopping events when there is high tide and high waves, but this does not mean there couldn't be wave overtopping when there is only high tide. Even though, we do not observe important increases in density that indicate an important saltwater input, so we cannot know when happens. Anyways, there are small changes in density both on the bottom and on the surface.

First, we observed density fluctuations at the surface but without causing important changes on February 14th, 16th, 19th, 20th, 26th, 27th and March 1st, while there was high tide and sometimes high waves, but all of them happened right after a wind event or during an increase of discharge (fig. 10), so we can't assume that one factor or another is causing it. Second, at the bottom we observed some density increases that were momentary on February 15th, 26th, 27th and 28th during high tide, and mainly noticeable in NM, which is the closest sensor to the sea. Those increases do not look like the increases in salinity caused by wind effects, because the salinity is bigger than the one before the wind event in some cases, although, as this still happens when there was a wind event we can't attribute it just to wave overtopping. Third, there was a continuous increase in DC at the bottom which is after an important decrease of salinity after a wind event.

5.2.2 Surface fluctuations controllers

If we focus on the depth at Pescadero we can observe more clearly how external factors are changing the estuary. The wavelet frequency analysis of depth is showing that between frequencies 0.01 and 0.001 Hz we can observe the effects of the waves into the lagoon, through identifying changes in its fluctuations and showing when there is presence of certain frequencies that could represent the ocean influence. If we crossed this information with tidal behavior and significant wave height we can obtain a more certain way to identify wave overtopping events.

We notice that when the estuary is open the ocean effects are very marked (Fig. 11). In closed state the effects are also evident but more slightly and we could point out that those are wave overtopping events. Also, we can say that they occur exclusively in high tide, and in any wave height, but the events are bigger when the waves are larger. On the other hand, wave overtopping does not have a clear pattern of behavior in dh/dt or in $(\hat{H}_{DC} - \hat{H}_{ML})/\Delta x$ when the inlet is closed.

As we notice earlier, discharge has two increase events during the studied period. We can observe that those increases are affecting directly to the surface, showing important peaks of dh/dt during those events (11). Also, the change of the standardized height in the horizontal showed at the beginning of the period negative values which changed to positive values after the increase of discharge, which result in happen after a big

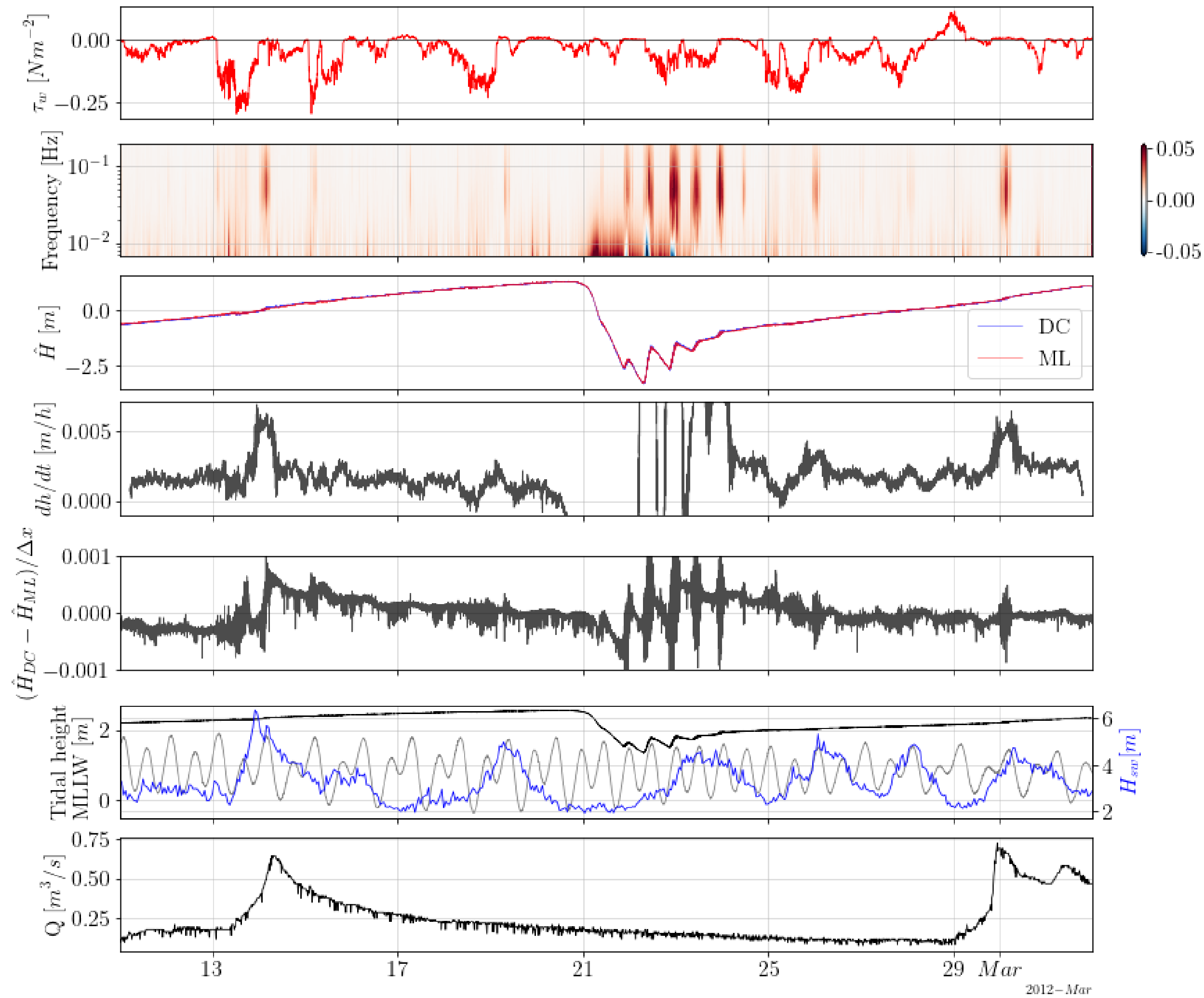

Figure 11: Time-series of wind stress (τ_w), depth wavelet frequency analysis at DC, standardized depth ($\hat{H}$) in DC, NM and ML locations, the change of the water level in a 10-hour frame (dh/dt), standardized depth change between locations DC and ML ($(\hat{H}_{DC} - \hat{H}_{ML})/\Delta x$), significant wave height in Halfmoon Bay (blue), Pescadero estuary water level (black) and tidal height in San Francisco (gray) in MLLW datum, and freshwater inflow of Pescadero creek (Q).

wind event and during a wave overtopping.

5.3 Wind-driven effects

As mentioned before, we noticed changes in density at the same time there were wind events, therefore for quantifying those events we calculated the potential energy anomaly of the water column in location NM and compared it to wind stress (Fig. 12), where we noticed that there were a lot of similarities between both time-series. We observed that when wind stress magnitude increases, potential energy anomaly decreases, except when there are positive values like on February 28th and 29th, when there was no change in potential energy anomaly. However, we can notice that the potential energy anomaly has not the same behavior in two wind events of the same magnitude, and we can observe that, in time, wind decreases its effect on the potential energy anomaly, only reaching 0 at the firsts wind events of each period. In addition, we can observe that after those events there is a decrease in potential energy anomaly when wind stress is zero, showing a change in their stratification structure after those events.

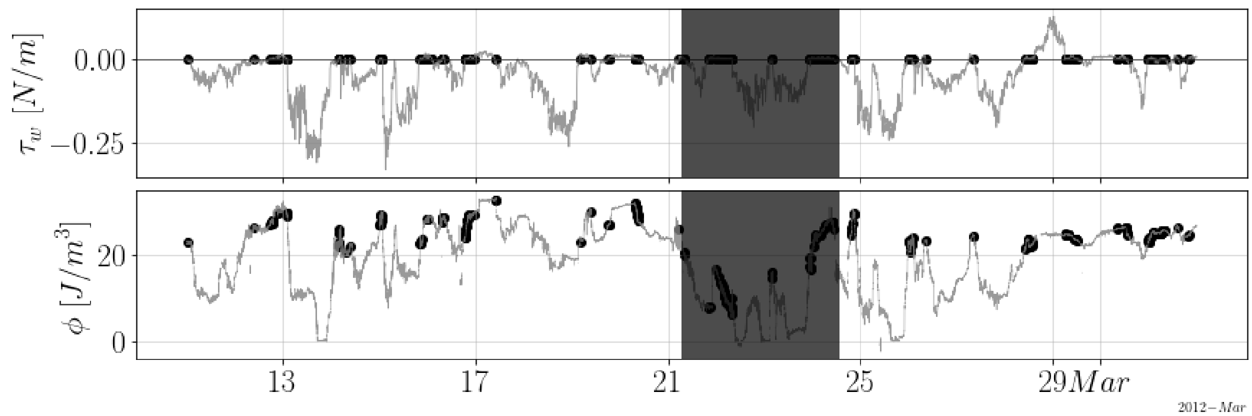

Figure 12: Time-series of wind stress (τ_w), and potential energy anomaly (ϕ). Dots are the instant when wind stress is zero. The shadowed window is when the estuary is in open state.

For further understanding, we implemented the Wedderburn number to observe if there was upwelling due to wind events. As we did not have the thickness of the epilimnion we estimated a range of positions for the pycnocline. This range started right after the first CTD, the deeper one (in black), and ended in the second CTD (in grey) (Fig. 13). Also, we marked with a star where was the epilimnion limit on February 16th which could be changing in time. As we are working with a range of values, we considered a partial upwelling when just the upper boundary reaches W=1 and full upwelling when both boundaries reach that value. In each period we noticed one full upwelling event and two partial upwelling events, for a total of six upwelling events observed in the studied period, always the first one being fully upwelled (Fig. 13). After full upwelling events, density at the bottom of the water column did not come back to its original values from before the event.

In Fig. 14 we can observe how density at the surface is getting more resilient to wind effects in time. The three wind events in the first period are similar in magnitude, but the increase in density that they make is each time smaller. What's more, we can notice a small increase in wind stress at the beginning of the time series that increase density three times more than the last wind event in the period. We can also notice that with the density changes in the vertical where at the first wind events of both periods reached 0 but after those started going steadier.

The first important wind event started on February 13th at 2 a.m. and the first location that was affected was NM, then ML, and finally DC. We can prove that with the change of density along the estuary (Fig. 14) where we observed negative values almost all the time, showing there are higher values in NM than in DC. When the wind starts to blow there is an increase of $\Delta\rho/\Delta x$ magnitude, and after reaching the peak the value decreases again to zero and stays there if the wind speed is constant. If wind speed decreases there is another increase in $\Delta\rho/\Delta x$ magnitude, showing that the wind stops influencing DC location first and then NM.

To quantify the time difference between the moment wind started blowing and density started changing at the different CTD locations, we calculate by visual inspection how long it took for the wind to affect density at

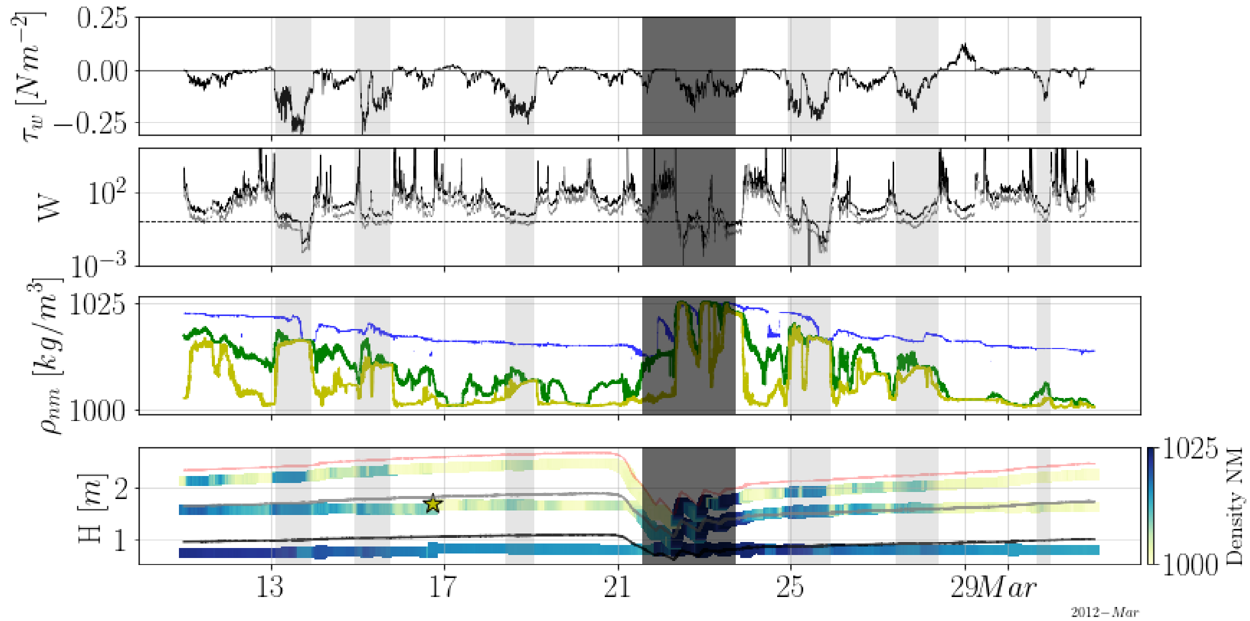

Figure 13: Time-series of wind surface shear stress (τ_w), Wedderburn number (W) where the dashed line shows W=1 and black and gray lines show W obtained at the lower and upper part of the selected window respectively, density at the bottom (blue), middle (green), and top (yellow) of the water column in NM location (ρ_{nm}) (see Fig. 7 for sensors positions), and colormap of density in time-space at each sensor of location NM with the black and gray line that limit the lower and upper part of the window of possible values for top layer width. The dark shadowed window is when the estuary is in open state. Light shadowed windows are when the upwelling events were observed. Red line is the water level, and the star indicates where the surface layer ends according to Fig. 7.

different points. To achieve this, we considered the moment that density just started to change into a trend after the wind started or stopped blowing. Also, to compare the obtained values we calculated the cross-correlation, between density and wind stress, after normalizing and standardizing both signals. We obtained the values of the first wind event, how long took to start and end, and for the cross-correlation we added the total of the first-period lag.

In Table 1 we observed that surface sensors (NM3, DC4, and ML2) had no delay with the cross-correlation method and did have it with a visual inspection. Also, at the latter, we observed that NM3 was the last sensor that started to change after wind stress started, but it increased faster than the others, fact that we can observe slightly in Fig. 14 for ρ_{top}. Also, we observed that the one that took longer to come back to its initial value was NM3, then ML2 and DC4.

If we compared Table 1 values to the response tilt time obtained as the fourth part of the internal wave period, that is 11.75 ± 2.72 min, we observe that it approximates the most to the values of the total period obtained by cross-correlation at the surface, but they are the double of it. Also, at the beginning of the event by visual inspection DC4 takes 10 minutes to start changing which, considering that DC is at the center of the estuary, could be the correct value.

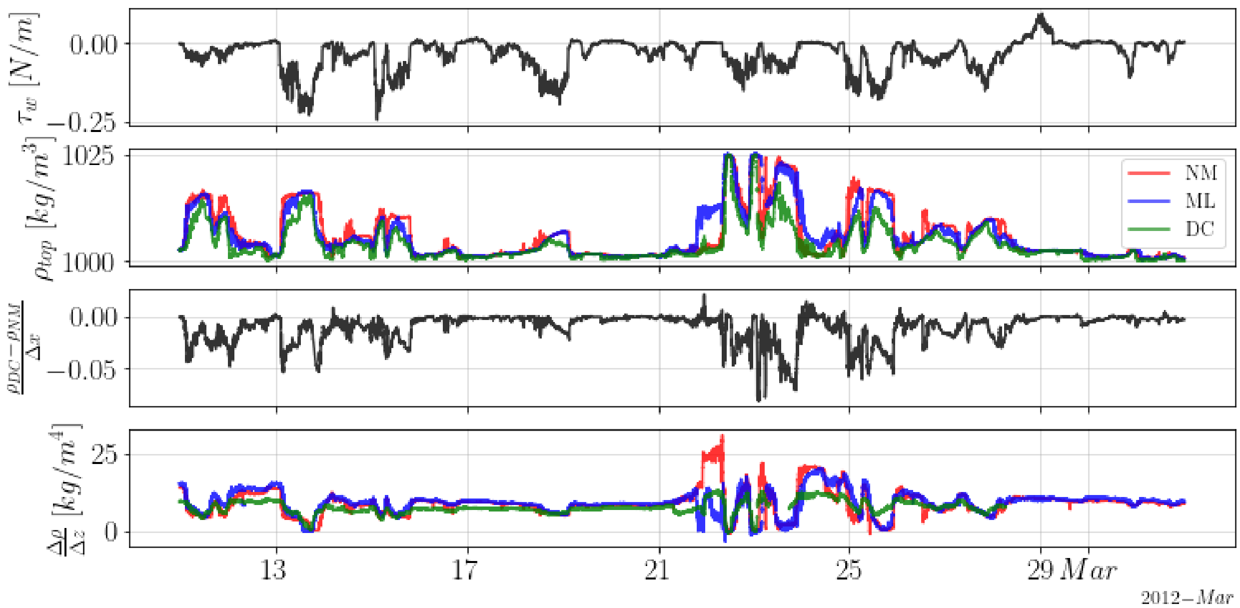

Figure 14: Time-series of wind shear stress at the surface (τ_w), surface densities in locations NM, ML, and DC (ρ_{top}), density change between locations DC and NM at the surface ($\frac{\rho_{DC}-\rho_{NM}}{\Delta x}$), and density change between surface and bottom in locations NM, ML, and DC ($\frac{\Delta\rho}{\Delta z}$ $[kg/m^4]$).

Surface wind stress over the closed estuary causes the upper layer to go in the same direction as the wind, and the lower layer to move in the opposite direction (Katopodes, 2019). Given the limitations of the ADCP sensor, velocities near the surface were not always captured, therefore, we observed a range of speed, not showing what happens at the bottom or the surface. On the other hand, Fig. 15 shows that as the wind increases, the along-estuary speeds (u) increase in a similar proportion, but in opposite direction. Wind is also influencing cross-estuary velocity (v), but in less intensity. Vertical velocity (w) present fluctuations and some negative or positive peaks during wind events or after in some cases.

The observed dynamic of the upper velocity at the window shown in Fig. 15 is such that when wind stress has positive velocity, considering positive the direction of the streamflow, the along-estuary water velocity is

Table 1: Lag obtained by cross-correlation method and visual inspection. Start columns mean that lag was calculated only when wind stress magnitude was increasing at the first event, and end columns mean that lag was obtained when wind stress magnitude was decreasing at the first event.

Method	Cross-correlation				Visual inspection		
Sensor	Start	End	Total event	Total period	Start	End	Total event
NM1	252 min	132 min	354 min	384 min	810 min	420 min	615 min
NM3	0 min	0 min	0 min	36 min	30 min	225 min	127 min
DC1	36 min	0 min	258 min	732 min	630 min	30 min	330 min
DC4	0 min	0 min	0 min	30 min	10 min	0 min	5 min
ML1	54 min	174 min	450 min	600 min	615 min	500 min	557 min
ML2	0 min	0 min	0 min	24 min	0 min	55 min	27 min

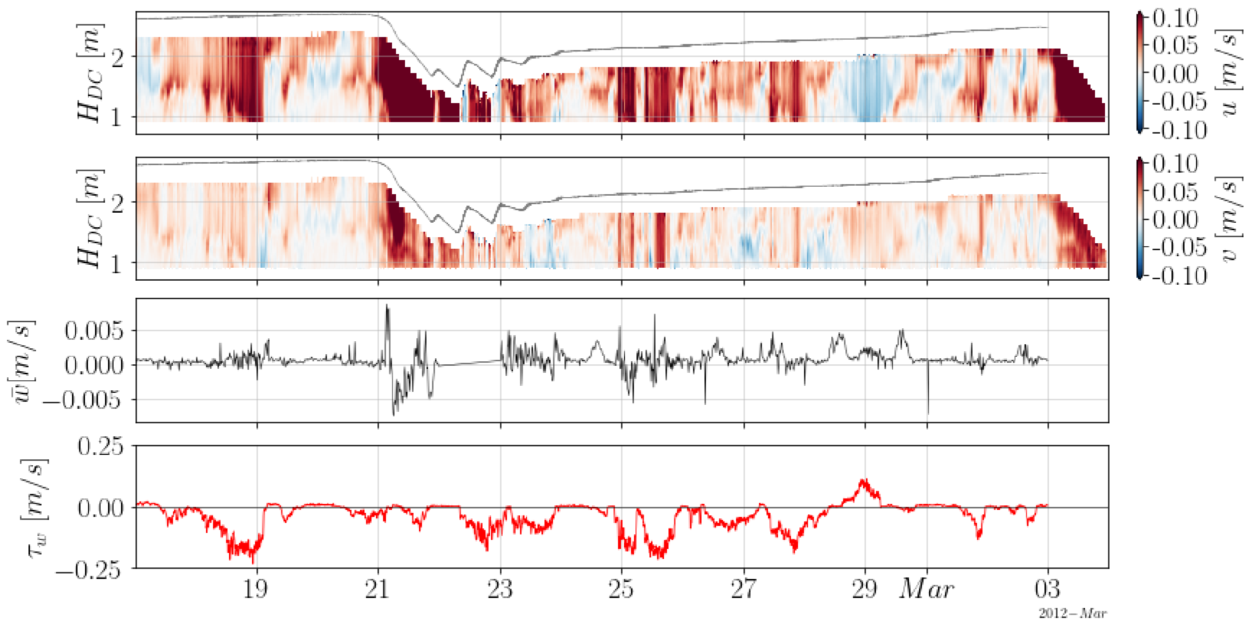

Figure 15: Time-series of u and v in the water column, averaged vertical velocity, and wind stress.

negative and vice versa. The magnitude of wind stress does not change this behavior along time, but as the water level increase, the estuarine velocity gets smaller for the same wind-stress magnitude. However, when wind stress is very small the dynamic change, and the upper along-estuary velocity at the window goes in the same direction as the wind stress at the surface.

For the average vertical velocity in the water column ($\hat{w}$) (Fig. 15), we can observe mainly positive direction (going up), but there is no interesting behavior in it until the second period when we observed more changes other than small fluctuations during a wind event. We could observe important peaks when the wind was starting to blow and, in some cases, right after the wind finished, showing that layers are going up at that moment. Also, we observed negative values during the first wind event on the second period, showing probably that the water column is returning to its initial place.

To observe in detail the behavior of the water column, densities and velocity profiles for each sensor were plotted in certain instants in the first wind event of the second period (Fig. 16). This wind event is characterized by two wind increases and a period in the middle with small wind stress that lasted 3 hours approximately. The profiles before the event, during the first increase, the middle period, the second increase, and after the event were plotted.

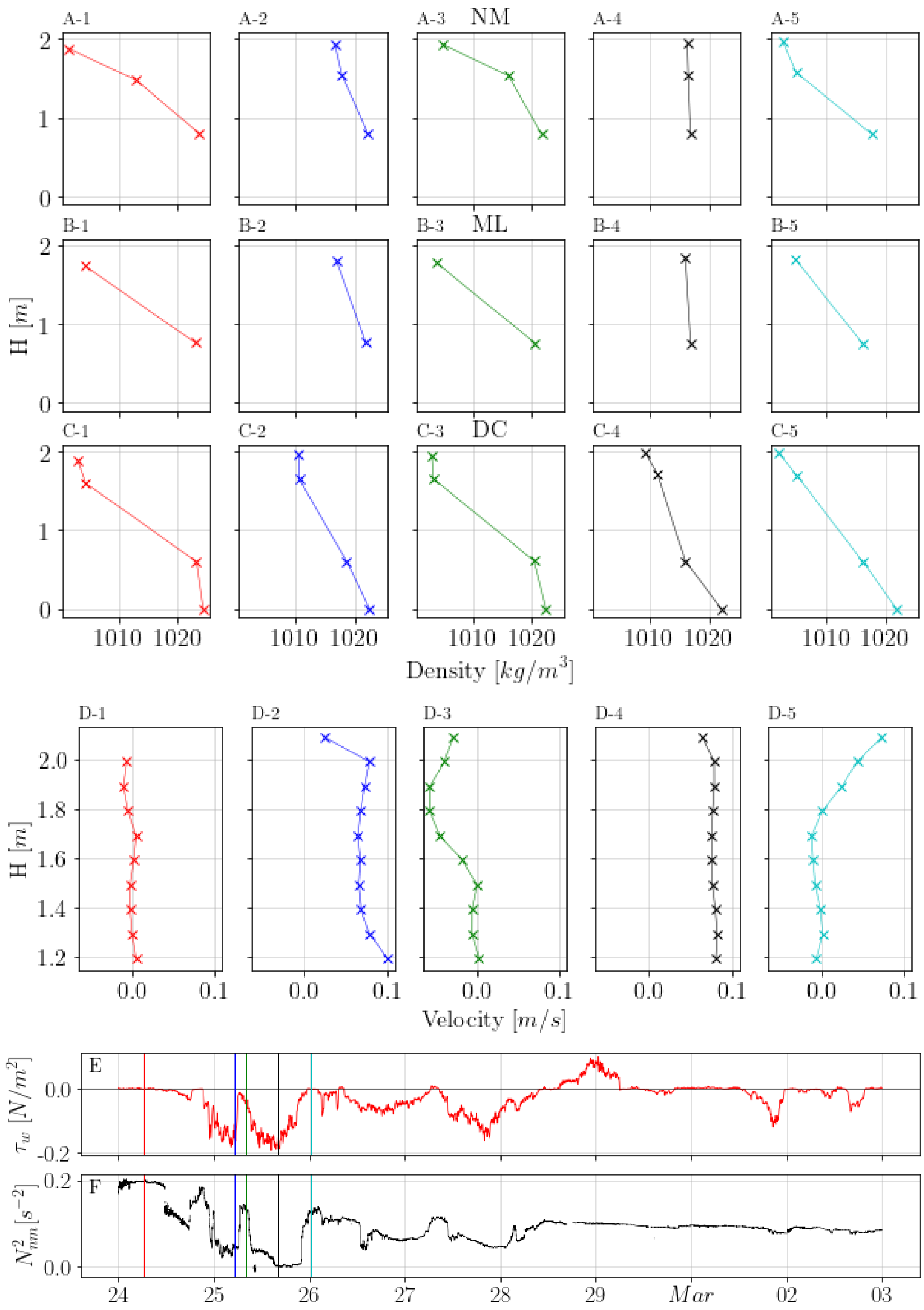

Figure 16: Density profiles at locations (A) NM, (B) ML and (C) DC, and (D) velocity profiles of 5 moments before, during, and after a full upwelling event, and time-series of (E) wind stress and (F) buoyancy frequency showing the instant of the profiles.

We could notice that before the wind event the water column is stratified, and the velocity is zero. During the first part of the event, the principal effect is the density increase near the surface and the positive velocity in all the visible part of the water columns. Then, when the wind stopped the estuary went stratified with similar values of density to the first profiles, but the velocity had a different behavior, and went negative in the upper layer, probably showing that the water is returning to its original state or that when wind stress is too small the surface water that goes into the same direction of the wind gets thicker and starts to be detected by the ADCP. When the wind reaches its maximum the water column is less stratified than in the first increase and velocity has bigger values. Finally, the last profiles show positive velocities at the surface and as there is no wind at that moment, maybe is showing the freshwater passing throw the estuary, also, the density profiles show a stratified estuary but less than before the event, meaning there was mixing in the water column during the wind event.

When the wind is blowing inland, shear stress causes a setup at the end of the estuary by driving water away from the free surface, increasing upstream hydrostatic pressure and causing estuarine recirculation. This causes the pycnocline to move towards the surface and increase in density where the surface layer used to be. This is what is happening in Fig. 16, where NM has been affected first and more abruptly than ML and DC, the latter being the one that changes its density the least. This may be because NM is the closest sensor to the mouth of the estuary, and therefore it is the one that detects the pycnocline first, followed by ML and DC.

On the other hand, buoyancy frequency values when wind stress is zero decreased, going from 0.2 to 0.1 kg/m^3 showing less stratification after the big wind event. Also, we can notice that N^2 is steadier after the wind event and decrease less for winds of the same magnitude (Fig. 16).

In Fig. 17 there is a closer look of the surface fluctuations behavior. First, in the wavelet analysis we observed three events of wave overtopping, which show a concentration of frequencies in the range from $2 * 10^{-2}$ to $2 * 10^{-1}$. Also, we observed that during the wind event the frequencies showed less concentration than in the wave overtopping event and was observed in the range of frequencies between 10^{-2} and $2 * 10^{-1}$. Second, the standardized height ($\hat{H}$) showed a peak when the wind started blowing, that after a while decreased to negative values with lots of surface fluctuations. When the wind stopped the height return to positive values near 0. This could be indicating that there is an inclination of the surface or a set up.

The change of the depth in time showed mainly positive values almost all the period (Fig. 17), meaning that the water level is increasing constantly. The only moment when the change was negative for more than an hour occur at the beginning of the wind event. Also, at the end of the time series there is a peak of negative values with unknown cause. The difference between the standardized height of DC and ML along-estuary indicates that when this value increases, the height in ML is smaller and the height in DC is bigger, and vice versa. This could be caused by both the wind and other external factors such as inflow from upstream, flow that may be entering or escaping through the sand bar, among others. In Fig. 17 at the beginning of the time series the values of $\Delta\hat{H}/\Delta x$ are oscillating slightly around 0. When the wind started blowing, the values turned negative, showing that DC decreased more than ML. After the wind event, the values continued the oscillations, but with more amplitude than before.

The spectral analysis of the depth in DC, ML and NM shows that between frequencies of $4 * 10^{-3}$ and 10^{-2} there is an increase in Power Spectral Density (PSD) (Fig. 18), showing us the presence of infragravity waves in Pescadero. If we add to the spectral analysis the wind stress and compare it we observed some similarities in the frequencies. Between $8 * 10^{-5}$ and 10^{-4} there is an increase in PSD for wind and depth at NM, that is

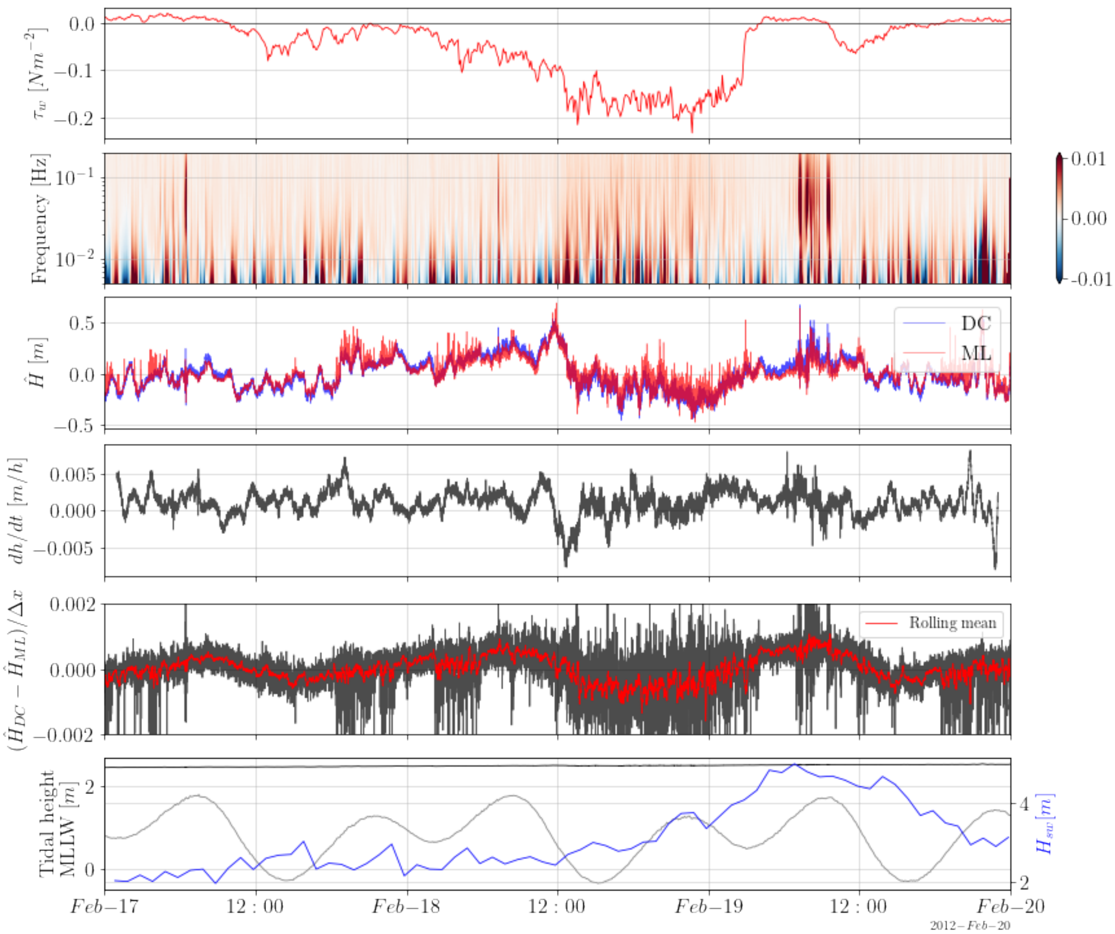

Figure 17: Time-series of wind stress (τ_w), depth wavelet frequency analysis at DC, standardized depth ($\hat{H}$) in DC and ML locations, the change of the water level in a 2-hour frame (dh/dt), standardized depth change between locations DC and ML (($\hat{H}_{DC} - \hat{H}_{ML})/\Delta x$) with its rolling mean, and significant wave height in Halfmoon Bay (blue), Pescadero estuary water level (black) and tidal height in San Francisco (gray) in MLLW datum.

for the period around 200 min, and also between 10^{-4} and $1.1 * 10^{-4}$ we notice peaks in wind and depth in ML and DC, that correspond to 140 min approximately.

References

Avalos Cueva, D., Monzón, C. O., Filonov, A., Tereshchenko, I., Limón Covarrubias, P., and Galaviz González, J. R. (2019). Natural frequencies of seiches in lake chapala. *Scientific reports*, 9(1):1–11.

Behrens, D. K., Bombardelli, F. A., and Largier, J. L. (2016). Landward propagation of saline waters following closure of a bar-built estuary: Russian River (California, USA). *Estuaries and coasts*, 39(3):621–638.

Behrens, D. K., Bombardelli, F. A., Largier, J. L., and Twohy, E. (2013). Episodic closure of the tidal inlet at the mouth of the Russian River—A small bar-built estuary in California. *Geomorphology*, 189:66–80.

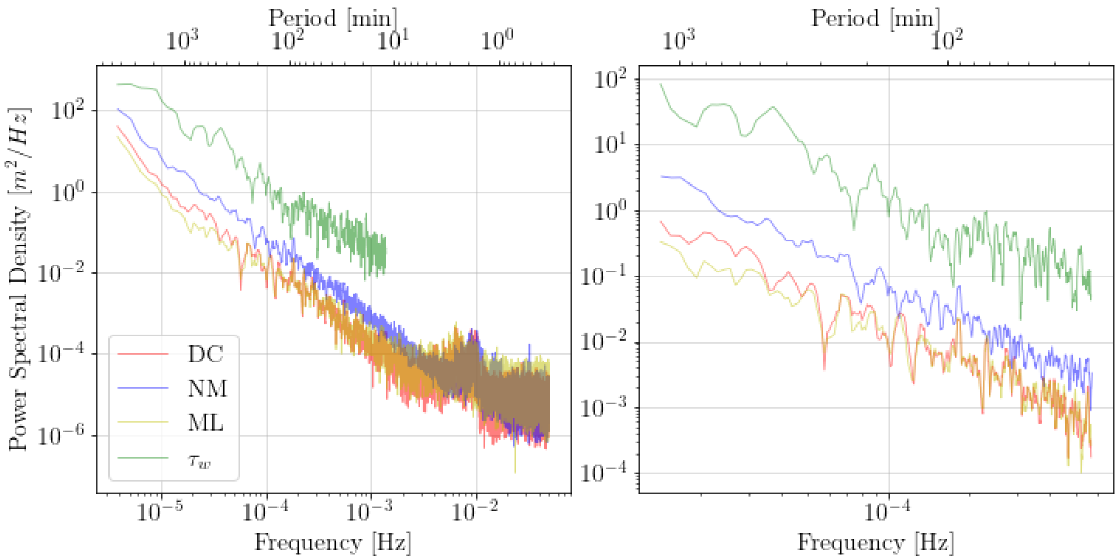

Figure 18: Frequency spectra of water level fluctuations in the estuary at sites in NM, DC and ML, and of wind surface stress between February 11th and 20th with a close up of the lower frequencies.

Clark, R. and O'Connor, K. (2019). A systematic survey of bar-built estuaries along the california coast. *Estuarine, Coastal and Shelf Science*, 226:106285.

Coman, M. A. and Wells, M. G. (2012). Temperature variability in the nearshore benthic boundary layer of Lake Opeongo is due to wind-driven upwelling events. *Canadian journal of fisheries and aquatic sciences*, 69(2):282–296.

Cousins, M., Stacey, M. T., and Drake, J. L. (2010). Effects of seasonal stratification on turbulent mixing in a hypereutrophic coastal lagoon. *Limnology and Oceanography*, 55(1):172–186.

Curry, R., Houghton, R., Kidwell, T., and Tang, P. (1985). Pescadero marsh management: A plan for persistence and productivity. *January*, 28:1985.

de la Fuente, A., Meruane, C., Contreras, M., Ulloa, H., and Niño, Y. (2010). Strong vertical mixing of deep water of a stratified reservoir during the maule earthquake, central chile (mw 8.8). *Geophysical Research Letters*, 37(24).

Dussaillant, A., Galdames, P., and Sun, C.-L. (2009). Water level fluctuations in a coastal lagoon: El yali ramsar wetland, chile. *Desalination*, 246(1-3):202–214.

Gale, E., Pattiaratchi, C., and Ranasinghe, R. (2006). Vertical mixing processes in intermittently closed and open lakes and lagoons, and the dissolved oxygen response. *Estuarine, Coastal and Shelf Science*, 69(1-2):205–216.

Hewitt, J. E., Ellis, J. I., and Thrush, S. F. (2016). Multiple stressors, nonlinear effects and the implications of climate change impacts on marine coastal ecosystems. *Global change biology*, 22(8):2665–2675.

Hoeksema, S. D., Chuwen, B. M., Tweedley, J. R., and Potter, I. C. (2018). Factors influencing marked variations in the frequency and timing of bar breaching and salinity and oxygen regimes among normally-closed estuaries. *Estuarine, Coastal and Shelf Science*, 208:205–218.

Holt, J., Wakelin, S., Lowe, J., and Tinker, J. (2010). The potential impacts of climate change on the hydrography of the northwest european continental shelf. *Progress in Oceanography*, 86(3-4):361–379.

Hordoir, R. and Meier, H. (2012). Effect of climate change on the thermal stratification of the baltic sea: a sensitivity experiment. *Climate Dynamics*, 38(9):1703–1713.

Jones, P. D., New, M., Parker, D. E., Martin, S., and Rigor, I. G. (1999). Surface air temperature and its changes over the past 150 years. *Reviews of Geophysics*, 37(2):173–199.

Katopodes, N. D. (2019). Chapter 11 - stratified flow. In Katopodes, N. D., editor, *Free-Surface Flow*, pages 780–839. Butterworth-Heinemann.

Kelly, S., de Eyto, E., Dillane, M., Poole, R., Brett, G., and White, M. (2018). Hydrographic maintenance of deep anoxia in a tidally influenced saline lagoon. *Marine and Freshwater Research*, 69(3):432–445.

Kundu, P. K. and Cohen, I. (2002). Fluid mechanics. sl.

Large, W. and Pond, S. (1981). Open ocean momentum flux measurements in moderate to strong winds. *Journal of physical oceanography*, 11(3):324–336.

Largier, J. (2021). Hydrological responses to closure in californian estuaries. In *Global Forum on Intermittent Estuaries*.

Largier, J., Aiello, I., Jacobs, D., Lacy, J., Pallud, C., Stacey, M., Carlson, S., Huber, E., and Bowles, C. (2015). Report of pescadero lagoon science panel. *Prepared for California State Parks*.

Laudier, N. A., Thornton, E. B., and MacMahan, J. (2011). Measured and modeled wave overtopping on a natural beach. *Coastal Engineering*, 58(9):815–825.

Laval, B. E., Morrison, J., Potts, D. J., Carmack, E. C., Vagle, S., James, C., McLaughlin, F. A., and Foreman, M. (2008). Wind-driven summertime upwelling in a fjord-type lake and its impact on downstream river conditions: Quesnel Lake and River, British Columbia, Canada. *Journal of Great Lakes Research*, 34(1):189–203.

Lee, G., Gommers, R., Waselewski, F., Wohlfahrt, K., and O'Leary, A. (2019). Pywavelets: A python package for wavelet analysis. *Journal of Open Source Software*, 4(36):1237.

Marti-Cardona, B., Steissberg, T., Schladow, S. G., and Hook, S. (2008). Relating fish kills to upwellings and wind patterns in the salton sea. In *The Salton Sea Centennial Symposium*, pages 85–95. Springer.

Martínez, M. L., Intralawan, A., Vázquez, G., Pérez-Maqueo, O., Sutton, P., and Landgrave, R. (2007). The coasts of our world: Ecological, economic and social importance. *Ecological economics*, 63(2-3):254–272.

McSweeney, S., Kennedy, D., Rutherfurd, I., and Stout, J. (2017). Intermittently closed/open lakes and lagoons: Their global distribution and boundary conditions. *Geomorphology*, 292:142–152.

National Data Buoy Center, N. (2022). Half moon bay standard meteorological data station 46012.

Neumann, B., Vafeidis, A. T., Zimmermann, J., and Nicholls, R. J. (2015). Future coastal population growth and exposure to sea-level rise and coastal flooding-a global assessment. *PloS one*, 10(3):e0118571.

Nunes, M. and Adams, J. (2014). Responses of primary producers to mouth closure in the temporarily open/closed great brak estuary in the warm-temperate region of south africa. *African Journal of Aquatic Science*, 39(4):387–394.

Omstedt, A., Pettersen, C., Rodhe, J., and Winsor, P. (2004). Baltic sea climate: 200 yr of data on air temperature, sea level variation, ice cover, and atmospheric circulation. *Climate research*, 25(3):205–216.

Peeters, F. and Kipfer, R. (2009). Currents in stratified water bodies 1: Density-driven flows.

Ranasinghe, R. and Pattiaratchi, C. (1999). The seasonal closure of tidal inlets: Wilson Inlet—a case study. *Coastal Engineering*, 37(1):37–56.

Ranasinghe, R. and Pattiaratchi, C. (2003). The seasonal closure of tidal inlets: causes and effects. *Coastal engineering journal*, 45(04):601–627.

Read, J. S., Hamilton, D. P., Jones, I. D., Muraoka, K., Winslow, L. A., Kroiss, R., Wu, C. H., and Gaiser, E. (2011). Derivation of lake mixing and stratification indices from high-resolution lake buoy data. *Environmental Modelling & Software*, 26(11):1325–1336.

Richards, C. M., Moal, O., and Pallud, C. (2018). Changes in water quality following opening and closure of a bar-built estuary (pescadero, california). *Marine Chemistry*, 198:10–27.

Roberts, D. C., Egan, G. C., Forrest, A. L., Largier, J. L., Bombardelli, F. A., Laval, B. E., Monismith, S. G., and Schladow, G. (2021). The setup and relaxation of spring upwelling in a deep, rotationally influenced lake. *Limnology and Oceanography*, 66(4):1168–1189.

Schernewski, G. (2002). *Baltic coastal ecosystems: structure, function and coastal zone management*. Springer Science & Business Media.

Schmidtko, S., Stramma, L., and Visbeck, M. (2017). Decline in global oceanic oxygen content during the past five decades. *Nature*, 542(7641):335–339.

Shintani, T., de la Fuente, A., de la Fuente, A., Niño, Y., and Imberger, J. (2010). Generalizations of the Wedderburn number: Parameterizing upwelling in stratified lakes. *Limnology and Oceanography*, 55(3):1377–1389.

Simpson, J. H., Brown, J., Matthews, J., and Allen, G. (1985). Tidal straining, density currents, and stirring in the control of estuarine stratification. *Estuaries*, 13:125–132.

Sloan, R. M. (2006). Ecological investigations of a fish kill in pescadero lagoon, california.

Stevens, C. and Imberger, J. (1996). The initial response of a stratified lake to a surface shear stress. *Journal of Fluid Mechanics*, 312:39–66.

Thorne, K. M., Buffington, K. J., Jones, S. F., and Largier, J. L. (2021). Wetlands in intermittently closed estuaries can build elevations to keep pace with sea-level rise. *Estuarine, Coastal and Shelf Science*, 257:107386.

Tides and Currents, N. (2022a). Monterey standard meteorological data buoy 9413450.

Tides and Currents, N. (2022b). San francisco standard meteorological data buoy 9414290.

U.S. Climate Data, N. (2021). Weather history for half moon bay.

Viaroli, P., Bartoli, M., Giordani, G., Naldi, M., Orfanidis, S., and Zaldivar, J. M. (2008). Community shifts, alternative stable states, biogeochemical controls and feedbacks in eutrophic coastal lagoons: a brief overview. *Aquatic Conservation: Marine and Freshwater Ecosystems*, 18(S1):S105–S117.

Water Data, U. (2022). Current conditions for usgs 11162500 pescadero creek.

Welch, P. (1967). The use of fast fourier transform for the estimation of power spectra: a method based on time averaging over short, modified periodograms. *IEEE Transactions on audio and electroacoustics*, 15(2):70–73.

Whitfield, A. and Bate, G. (2007). A review of information on temporarily open/closed estuaries in the warm and cool temperate biogeographic regions of south africa, with particular emphasis on the influence of river flow on these systems. *Water Research Commission, Report*, 1581(1):07.

Williams, J. et al. (1990). Pescadero marsh natural preserve hydrologic enhancement plan. *San Francisco, CA*.

Williams, M. (2014). Hydrodynamics and salt dispersion in intermittently closed bar-built estuaries.

Williams, M. and Stacey, M. T. (2016). Tidally discontinuous ocean forcing in bar-built estuaries: The interaction of tides, infragravity motions, and frictional control. *Journal of Geophysical Research: Oceans*, 121(1):571–585.

Winckler, P., Aguirre, C., Farías, L., Contreras-López, M., and Masotti, Í. (2020). Evidence of climate-driven changes on atmospheric, hydrological, and oceanographic variables along the chilean coastal zone. *Climatic Change*, 163(2):633–652.

Winckler Grez, P., Aguirre, C., Farías, L., Contreras-López, M., and Masotti, Í. (2020). Evidence of climate-driven changes on atmospheric, hydrological, and oceanographic variables along the chilean coastal zone. *Climatic Change*, 163(2):633–652.

Woolway, R. I., Meinson, P., Nõges, P., Jones, I. D., and Laas, A. (2017). Atmospheric stilling leads to prolonged thermal stratification in a large shallow polymictic lake. *Climatic Change*, 141(4):759–773.

Wüest, A. and Lorke, A. (2003). Small-scale hydrodynamics in lakes. *Annual Review of fluid mechanics*, 35(1):373–412.